



Investigation of soil characterization in Hatay Province in Turkey by using Seismic Refraction, Multichannel Analysis of Surface Waves and Microtremor

Cengiz Kurtuluş, İbrahim Sertçelik*, Fadime Sertçelik, Hamdullah Livaoglu, Cuneyt Saş
Kocaeli University, Department of Geophysics, Kocaeli, 41100, Turkey

*Corresponding author: isert@kocaeli.edu.tr

ABSTRACT

In this study, shallow seismic surveys, including seismic refraction, Multichannel Analysis of Surface Waves (MASW), Refraction Microtremor (ReMi), and Microtremor measurements were conducted to estimate site characterization at 26 strong-motion stations of AFAD (Disaster and Emergency Management Presidency) in the province of Hatay, situated in one of the most seismically active regions in southern Turkey. The Horizontal to vertical spectral ratio (HVSr) technique was applied, using smoothed Fourier spectra derived from a long duration series to determine dominant frequency values at different amplification levels. Shear wave velocity up to 30 m of the ground was detected with MASW analysis. In the ReMi analysis, up to 80 m was reached with a corresponding average of 650 m/s shear wave velocity. The shear wave velocities estimated by the MASW method up to 30 m were compared with those found by the ReMi method, and they were observed to be very compatible. The province of Hatay was classified according to Vs30 based NEHRP Provisions, Eurocode-8, the Turkish Building Earthquake Regulation (TBDY-2018), and Rodríguez-Marek et al. (2001). The shear-wave velocity (Vs30), Horizontal to Vertical ratio's (H/V) peak amplitude, dominant period, and site class of each site were determined. The H/V peak amplitudes range between 1.9 and 7.6 while the predominant periods vary from 0.23 sec to 2.94sec in the study area. These results are investigated in order to explain the consistency of site classification schemes.

Keywords: Soil investigation; MASW; ReMi; HVSr technique; Site Classification.

Caracterización del suelo en la provincia de Hatay, Turquía, a través de los métodos Refracción sísmica, Análisis Multicanal de Ondas Superficiales y Microtemblores

RESUMEN

En este trabajo se realizaron sondeos sísmicos superficiales como la refracción sísmica, el Análisis Multicanal de Ondas Superficiales (MASW, del inglés Multichannel Analysis of Surface Waves), la refracción de microtemblores (ReMi, del inglés Refraction Microtremor), y la medición de microtemblores para una caracterización en 26 estaciones de registros sísmicos de la AFAD (Autoridad para la Administración de Desastres y Emergencias) en la provincia de Hatay, que está situada en una de las regiones sísmicamente más activas del sur de Turquía. Se aplicó la técnica de Relación Espectral Horizontal a Vertical con un espectro Fourier regular derivado de una serie de larga duración para determinar los valores de frecuencia dominante a diferentes niveles de amplificación. La velocidad de la onda de corte por encima de los 30 metros de profundidad se detectó a través de la técnica MASW. El análisis ReMi por encima de los 80 metros se logró con una media correspondiente de 650 m/s en la velocidad de la onda de corte. Las velocidades en las ondas de corte alcanzadas por el método MASW se compararon con aquellas de la técnica ReMi, y se observó que son muy compatibles. La provincia de Hatay fue clasificada de acuerdo con la norma NEHRP con base en Vs30, Eurocode-8, la entidad de regulación sísmica de Turquía (TBDY-2018), y Rodríguez-Marek et al. (2001). Se determinó la velocidad de la onda de corte (VS30), la amplitud del pico de la relación Horizontal a Vertical (H/V), el período dominante, y el tipo de cada sitio analizado. Las amplitudes del pico en las relaciones H/V están entre 1.9 y 7.6, mientras que los períodos predominantes varían entre 0.23 segundos y 2.94 segundos en el área de estudio. Estos resultados se investigaron para explicar la consistencia de los esquemas de clasificación de sitios.

Palabras clave: Investigación del suelo; MASW; ReMi; Técnica de Relación Espectral Horizontal a Vertical; clasificación de sitio.

Record

Manuscript received: 15/04/2019
Accepted for publication: 07/08/2020

How to cite item

Sertçelik, I., Kurtuluş, C., Sertçelik, F., Livaoglu, & Saş C. (2020). Investigation of soil characterization in Hatay Province in Turkey by using Seismic Refraction, Multichannel Analysis of Surface Waves and Microtremor. *Earth Sciences Research Journal*, 24(4), 473-484. DOI: <https://doi.org/10.15446/esrj.v24n4.79123>

Introduction

The Hatay area is located in a seismically active region at the western end of the 1000-km long border formed by Arabic and Turkish plates. The tectonic activity of the region shows a complex tectonic behavior under the influence of faults extending to the Dead Sea, Eastern Anatolia, and Cyprus (Beyen et al., 2003). More than ten of the most disastrous earthquakes during the past century (1937–2015) occurred in this area, indicating that local site conditions have a major effect on ground shaking. It was reported that the tsunamis that occurred during the 1822 and 1872 earthquakes in Hatay caused the death of 20 thousand people (Tan et al., 2013). These devastating earthquakes from the past have shown that local ground condition is a major influence on ground amplification which can be calculated by a S-wave velocity structure and microtremor studies. There have been several site effect studies in the forms of a microtremor survey, earthquake observations, a surface-wave survey, and borehole data for various regions in Turkey such as Bayülke (1982), Erdik (1984), Ambraseys et al. (1993), Inan et al. (1996), Aydan & Hasgör (1997), Durukal et al. (1998), Zaré & Bard (2002), Ozalaybey et al. (2002), Rathje et al. (2003), Ergin et al. (2004), Kalafat et al. (2007), Sandikkaya (2008), Sandikkaya et al. (2010), Kalkan & Gürkan (2004), Ulusay et al. (2004), and Yılmaz et al. (2008). Zaré & Bard (2002) used a (H/V) spectral ratio to estimate Turkey's strong motion site conditions, and Rathje et al. (2003) and Gülkan et al. (2007) used geophysical and geotechnical studies to determine the site classification of Turkish strong-motion sites. Many local site investigations have been conducted by many researchers in Turkey (Kurtuluş et al., 2016; Ongun, 2010; Alçık et al., 1995; Dikmen & Mirzaoglu, 2005). However, only a few studies about site effect were performed in the Hatay region. Büyüksaraç et al. (2014) conducted a site response analysis, compiling data such as density, seismic wave velocity, and soil cross-sections from previous seismic microzonation studies and acceleration data from four free-field strong-motion stations of the SERAMAR project. They determined three different layers for the ranges 0-5 m, 5-15 m, and 15-25 m. The seismic velocities of these layers vary between 380 and 470 m/s for 0-5 m, 320 and 480 m/s for 5-15m, and 470 and 750m/s for 15-25m. Over et al. (2011) analyzed the microtremor data for Antakya and proposed a preliminary microzonation map for the province of Antakya based on dominant periods ranging from 0.2 to 0.8 sec and shear wave velocities of the sediments covering the area. Korkmaz (2006) studied the relationship between ground conditions and earthquake effect in Antakya. Horoz (2008) studied the seismicity of the region between Adana-Antakya-Kahramanmaraş with the parameter "b" and risk analysis. Ceken & Polat, (2014) tried to investigate local site effects with MATNet installed near the Hatay-Kahramanmaraş areas, consisting of 55 triaxial force-balance accelerometers and capable of recording explosions and evaluating them as a part of an early warning and preliminary damage estimate system. Ozmen et al., (2017) conducted a microtremor array exploration of shallow S-wave velocity profiles at 28 sites in the provinces of Hatay and Kahramanmaraş. They determined fundamental frequencies from 0.8 to 10 Hz in Hatay and peak amplitude values of more than 5 in Kahramanmaraş. There is also site predominant based seismic site classifications regarding sediment thickness carried out by researchers which promising reliable preliminary results (Livaoglu H., & Irmak T.S., 2017; Livaoglu, H., & F. Sertçelik, 2017). They have used the strong ground motion data and evaluated the site predominant periods of the installed stations via response spectra of H/V.

In this study of seismic refraction, Multichannel Analysis of Surface Waves (MASW), a refraction microtremor (ReMi) and single station microtremor studies were conducted at 26 strong-motion stations of AFAD located in the province of Hatay to investigate S-wave velocity distribution in shallow soil which is important in the design of seismic hazards.

Geology and tectonics of the region

Hatay and its surrounding are located to the south of the Antakya-Kahramanmaraş graben, which developed under the influence of the Dead Sea and Eastern Anatolian Faults and the Cyprus Spring. The south of the graben is shaped by the Dead Sea Fault. However, Arabian and African plates move northward under the influence of convective currents in the mantle over the weakly resistant (fluid) upper asthenosphere. The slip vectors of earthquakes in

the region, the fault systems, the global kinematic models based on the oceanic spread, indicate that the Arabian plate moves north-northwest to Eurasia at an average speed of 25 mm per year. The African plate is moving northward at about 10 mm per year in relation to Eurasia (Reilinger, et al.1997). Although many destructive depressions have been exposed in the historical period, there has not been an earthquake in the area for 135 years. This situation increases the risk of destructive earthquakes every day (Fig. 1). The Otokton Arabian platform rocks with the main lines of the geology of the Amanos Mountains covering the vast majority of the region; Ophiolite nappes; Neo-autoclaved sediments covering nappes and autochthonous units are defined. The Amanos Mountains located at the southern tip of the Eastern Taurus Mountains and the Kızıldağ ophiolite massif in the vicinity of them also have an important place in the geology of the region (Fig. 2).

Data acquisition and analysis

Seismic refraction, MASW, REMI, and single station microtremor data were collected at AFAD's 26 strong motion stations in the province of Hatay in southern Turkey. The seismic refraction data were recorded for 2.0 sec with a sampling rate of 1.0 msec using a 50 kg weight-dropping energy source with a hydraulic weight-lifting unit operated by a battery powered electric motor. Number of 48 P- wave geophones with 4.5 Hz were fixed in line form at 2.0 m intervals (Fig. 3).

Data were collected from forward, midpoint, and reverse shootings with two m offsets; transferred to 48 channels GEODE recording units; and converted from analog to digital form. The midpoint of the geophone spread was placed as close as possible to the strong motion station on a flat area so that the static corrections of the shot and geophone points were neglected. An example of the shot records obtained at Station 3112 is shown in Figure 4a. The first arrival times of the refracted P-waves were picked from the field record, and the corresponding travel time-distance curves of the profile were determined (Figure 4b). The initial P-wave velocity-depth model was then obtained from the first arrival times. Then, this initial model was processed iteratively by nonlinear travel time tomography (Zhang & Toksöz, 1998) to obtain the final P-wave velocity-depth model. Iteration was stopped when the differences between the first arrival times and the modeled were reduced to an acceptable minimum value as 8. The P-wave velocity-depth cross-section of the site was determined laterally averaging the P-wave velocity-depth model (Fig. 4c).

Shot records on both sides were used in the analysis of Multichannel Analysis of Surface Waves (MASW) to estimate the Vs profiles of the top 30 m. It was observed that layers varying in thickness from 5m to 18m up to 30m. The shot record was isolated from the refracted by muting before and after. Low and high frequency noises were filtered through a bandpass filter with frequencies (2, 4, 36, 48) Hz (Figure 5a). Thereafter, plane wave decomposition was applied to convert the data from the offset time to the phase velocity versus the frequency domain (Park et al., 1999; Xia et al., 1999). The dispersive curve related to a fundamental mode of surface waves was picked from this domain. The S-wave velocity was determined as a function of depth by inverting the dispersion curve. It has been observed that each frequency component of Rayleigh waves propagates at different phase velocities; in other words, these waves have scattering properties on the ground. The greatest share of the energy of the Rayleigh waves belongs to the fundamental mode, although not for every case. For this mode, dispersion curve representing the change of the phase velocity relative to the frequency is determined. This dispersion curve was used to determine the S-wave velocity-depth profile of the stationary region by inversion method (Fig. 5b). The dispersion curve for the basic mode showing the change of the frequency and the phase velocity is shown in Figure 5c.

A ReMi study was performed to check the velocity-depth profile obtained by the MASW method at a depth of up to 30 m as well as to find the velocity-depth profile at the lower half of 30m. The ReMi data were recorded for 32 sec with 2.0 msec sampling rate in the same field layout using ambient noise from wind and traffic as a seismic source. 24-25 records were stacked in each ReMi installation to remove the cultured noise from the microtremor data at each site. Rayleigh waves are distinguished from other waves by using two-dimensional slowness frequencies (p-f) transformations of noise records spreading in both directions. The Rayleigh wave dispersion is selected along the minimum velocity envelope of energy in the spectral image of the slowness frequency.

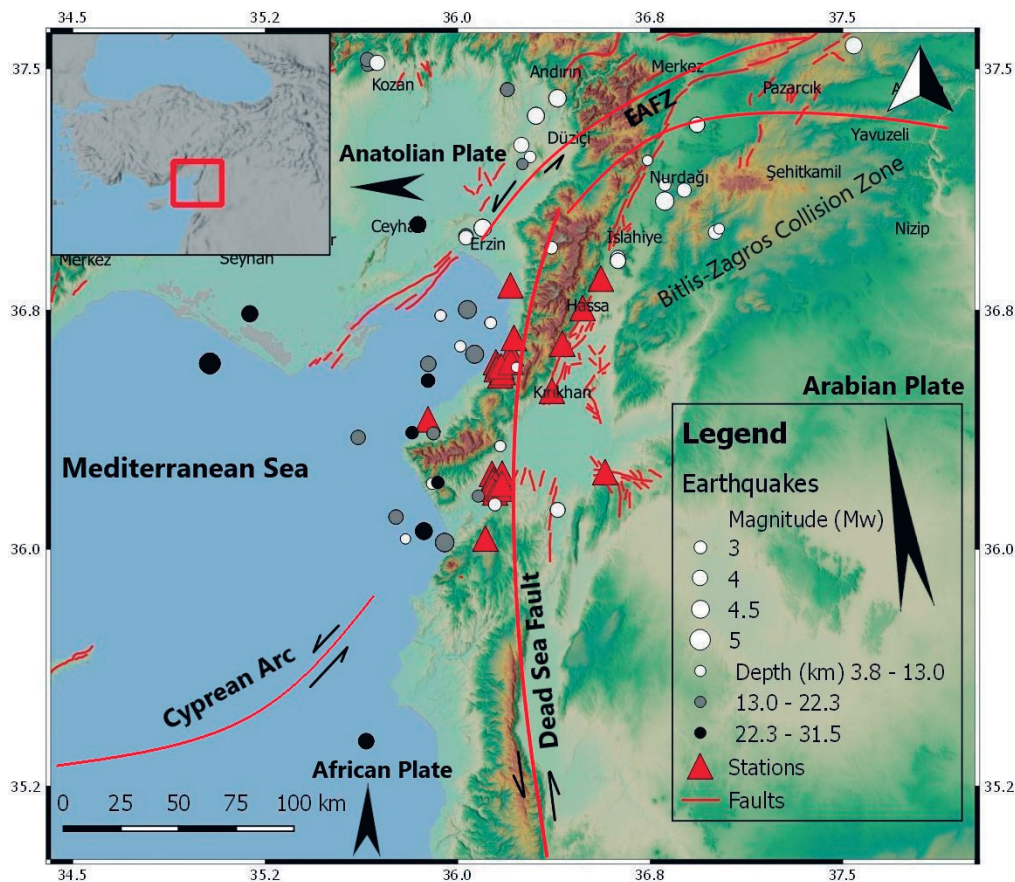


Figure 1. Tectonics of the study area, location of stations and epicenter of the earthquakes that have taken place in the last 10 years. Thick black dash arrows shows the plate’s movements. Red triangles shows the stations. The colored circle points shows the earthquakes according to their magnitudes and depths

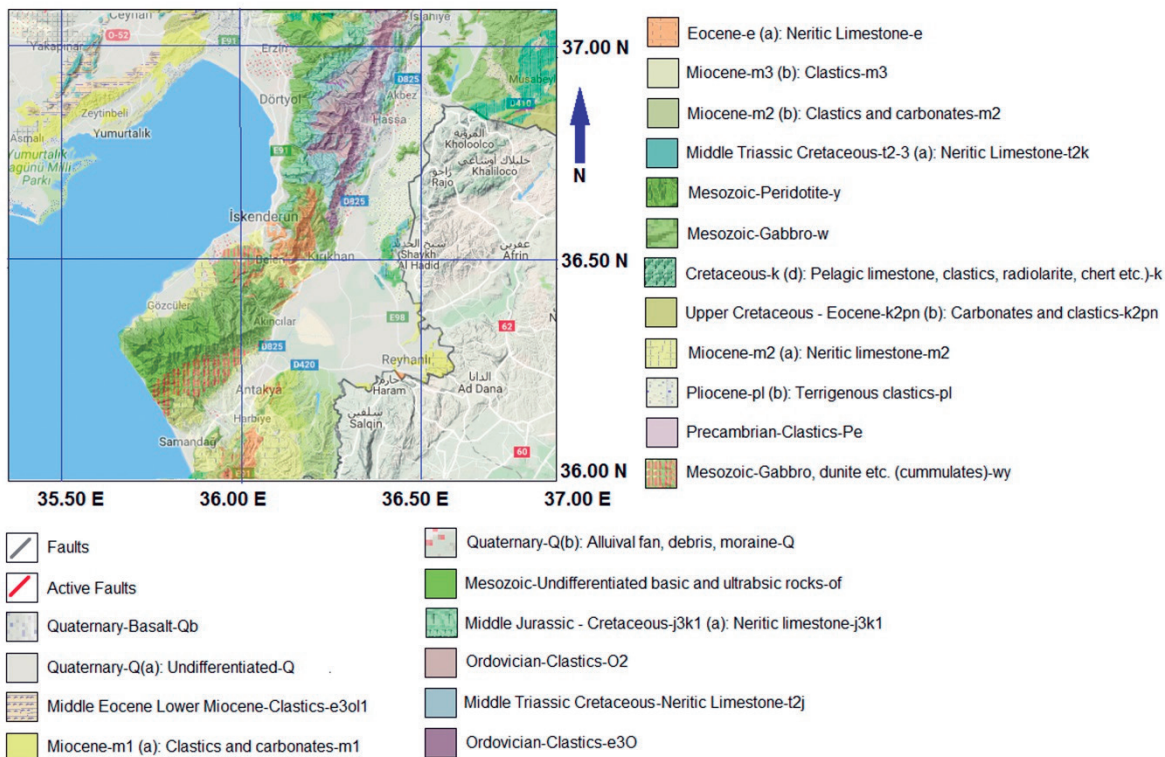


Figure 2. The geology map of the study area (Emre et al., 2013; Akbaş et al.,2002a).

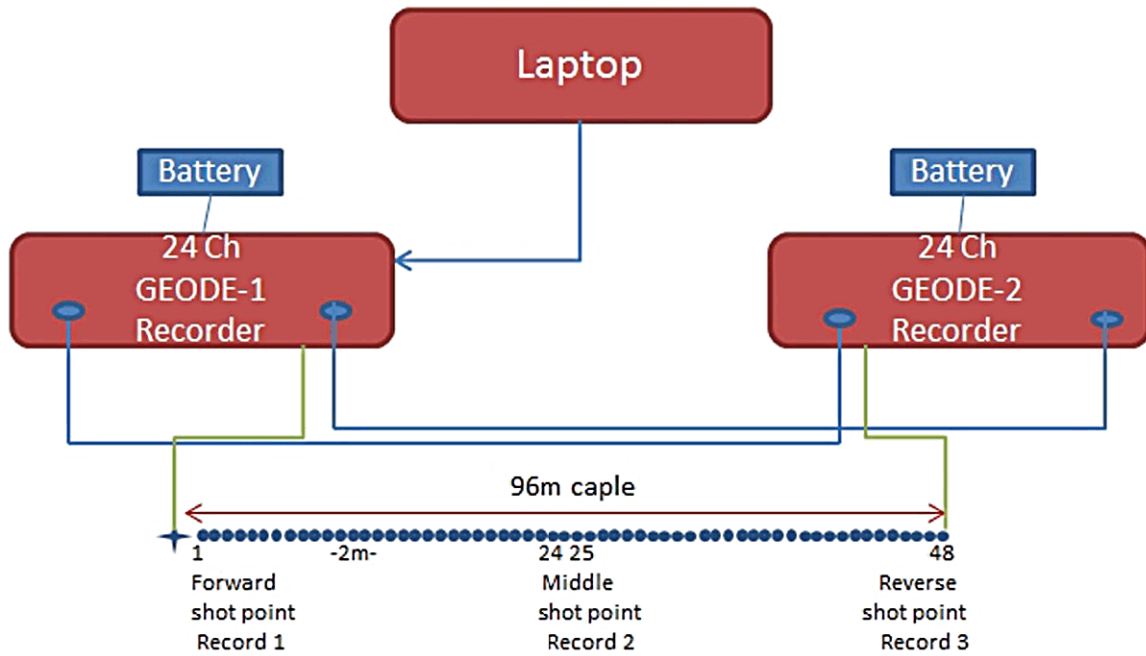


Figure 3. MASW acquisition data scheme with a 48-channel linear receiving array

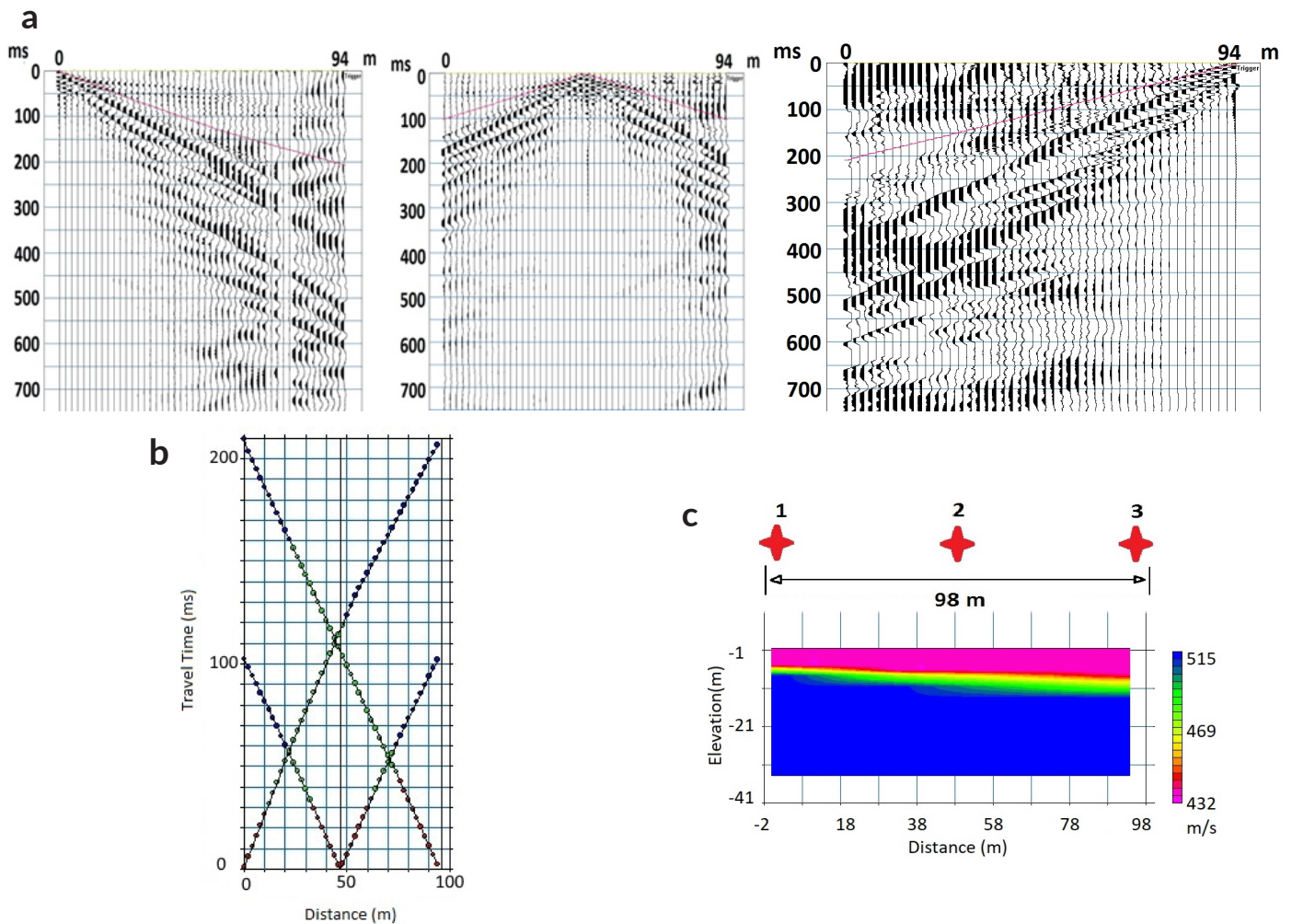


Figure 4. Sample seismic refraction record taken at the station coded 3112. (a) seismic refraction records with picked first arrival times showing as a red line, (b) observed and calculated travel time curves, (c) P-wave velocity-depth model along the profile

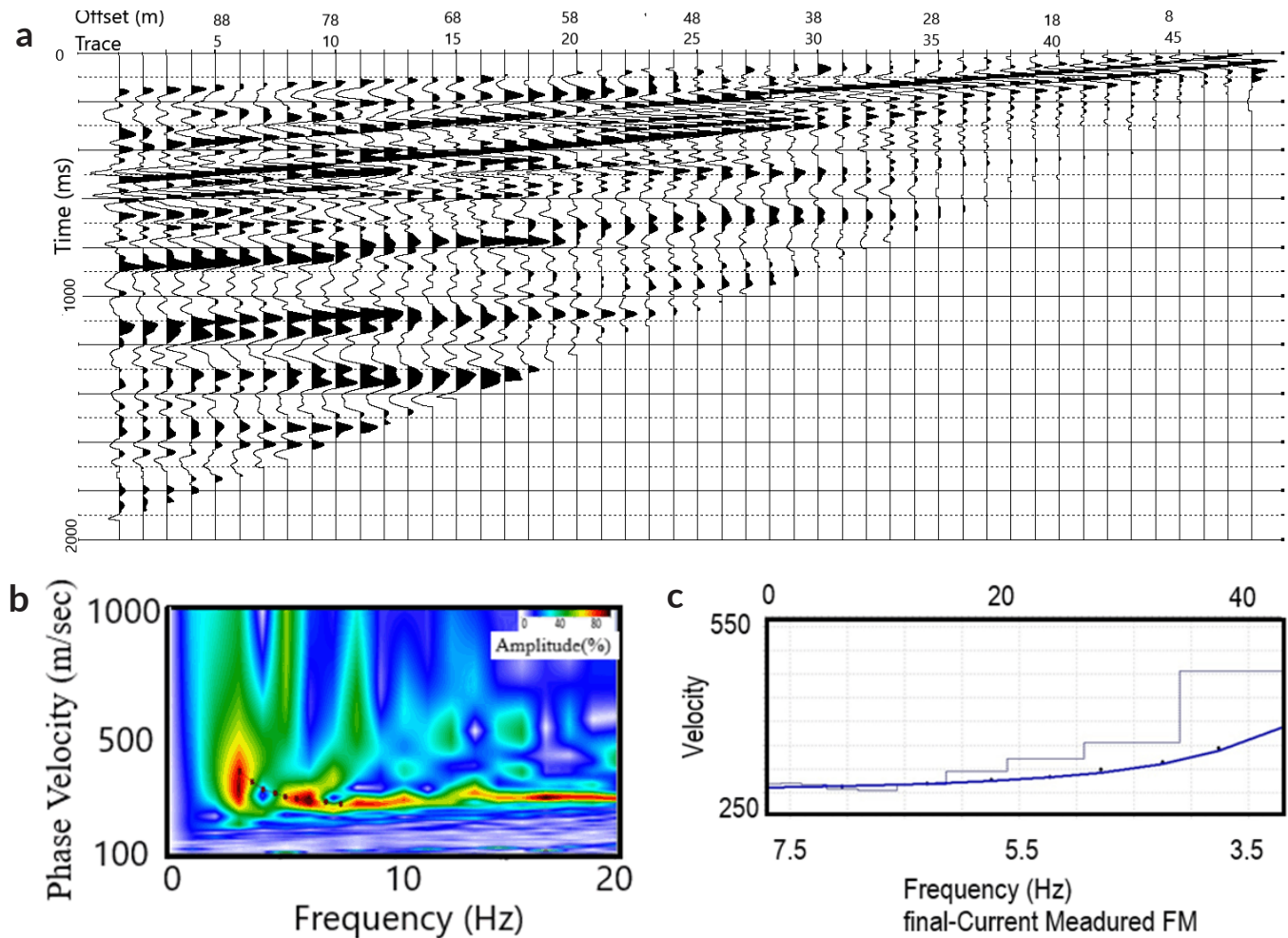


Figure 5. (a) The shot record separated from the refraction and reflected waves at the station coded 3112, (b) Phase velocity-frequency and picking dispersion curve, (c) Vs-depth profile and modeled dispersion curve. The S-wave-depth profile (blue) and the modeled dispersion curve (black).

The spectrum is normalized as the ratio of the power spectrum at certain frequency slowness over the mean slowness values of that frequency. The best way to obtain accurate phase velocities is to choose the fundamental mode phase rate of the Rayleigh wave dispersion along the minimum edge of the vertical steep slopes of the dispersion curves (Louie, 2001). These Rayleigh wave dispersion picks are modeled using the experiment and error settings of the velocity-depth model to determine the shear wave velocity-depth profile. The time-distance data are shown in Fig. 6a. The dispersive curve for the fundamental mode of surface waves are transformed to frequency- phase velocity domain to pick fundamental dispersion curve (Fig 6b) and is inverted to obtain the S-wave velocity depth profile (Fig. 6c).

A velocity based broad-band sensor (flat response between 0.03-50 Hz) was used for ambient noise recording. Whole data were acquired with the same sensor. (Figs. 7a and 7b). The estimated spectra of the three components microtremor data are given in Fig. 8c. The H/V amplitude spectrum of dominant frequency and amplification of the 3112 coded station are given in Fig. 7c. As seen from Fig.7c, the dominant frequency of the ground is 5 Hz (period is 0.2 sec.) and H/V ratio or peak amplitude at this frequency is 6.6.

The theoretical H/V amplitude spectra of the stations were also calculated to check the validity of the observed values. The theoretical amplification functions of stratified soil layers (Table 1) were calculated according to the recursive algorithm proposed by Tsai (1970) and modified for calculations (see also Tsai and Housner, 1970, Herak, 2008). The theoretical amplification functions of stratified soil layers (Table 1) were calculated according to the recursive algorithm proposed by Tsai (1970) and modified for code (see also Tsai & Housner, 1970, Herak, 2008). The H/V transfer functions were

synthetically derived for the station 3112 as shown in Fig. 8. Observed H/V curve were also estimated from the microtremor measurements for the 3112 coded station.

The values from the table 1 are in-situ measurements and results from the field near the stations. It can be clearly seen from the figure that the fundamental peak frequency corresponding to the H/V amplitudes are in step with each other which indicate 2.55 and 3.17 Hz respectively which are in the similar site class for predominant based site classifications. The significant difference between the fundamental frequencies and H/V amplitudes of the site could be originated from lateral irregularities. Besides, the fundamental peak frequency corresponding to the H/V amplitudes are compatible. The shear wave velocities, $V_{s_{30}}$, soil classes, H/V peak amplitudes, and dominant soil periods are given in Table 2.

Where V_p and V_s are respectively the P and S- wave velocities, Q_p and Q_s are the quality factors related with P-and S-velocities, ρ is density, and h indicates the layer thickness.

Sites utilizing the information obtained from shallow field tests are classified according to BSSC (2003), CEN (2003), TBDY (2018), and Rodriguez-Marek et al. (2001), all of which recommend criteria based on the average shear wave velocity $V_{s_{30}}$ of the top 30 m soil/rock profile. The mean shear wave velocity of the uppermost 30 m at a site is calculated by

where d_i and V_s are respectively the thickness, shear wave velocity of the i^{th} layer, and n is the number of layers in the top 30 m. The V_s profile obtained from the MASW measurements is used to compute the $V_{s_{30}}$ for each strong motion station. Velocity-depth values obtained by MASW up to 30m depth are in good agreement with the values found by the ReMi method.

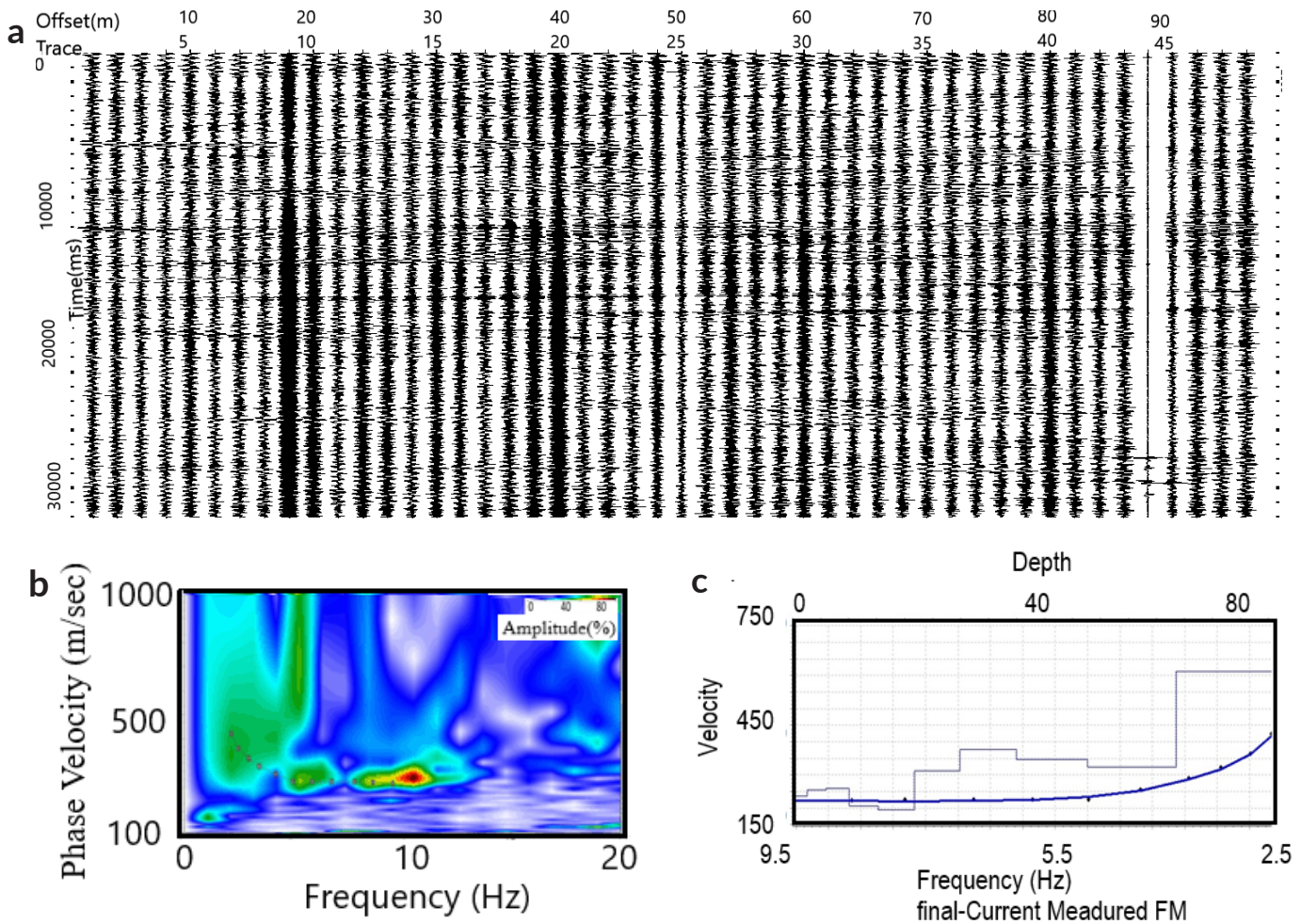


Figure 6. (a) ReMi data, x-t domain at the station coded 3112, (b) the dispersion spectrum calculated by separating the plane-wave components of the surface waves present in the seismic record, (c) ReMi S-wave velocity-depth profile (blue) and modeled dispersion curve (black). The vertical axis indicates the S-wave velocity and the horizontal axis shows the frequency of dispersion curve.

Site classification according to NEHRP provisions

The NEHRP recommends six field classes (A, B, C, D, E, and F) for identifying site-specific design spectra, shown in Table 3.

Based on $V_{s,30}$, eight of the 26 sites are classified as Class D, 16 as Class C and two as Class B. In other words, 30.7% of the total places correspond to Class D, 61.5% to Class C, and 7.69% to Class B.

Site classification according to Eurocode-8

The field classification scheme proposed by Eurocode-8 is quite similar to the NEHRP provisions (Table 4). The difference between the two is that the A and B classes of the NEHRP provisions are included in Eurocode-8 as Class A. In addition, the limit of 760 m/s between the A and B classes in the NEHRP provisions is set to 800 m/s in Eurocode-8.

According to Eurocode-8, eight sites correspond to Class C (30.77%), 17 to Class B (65.38%), and one to Class A (3.84%). As can be seen, Classes D, C, and B in the NEHRP provisions correspond to Classes C, B, and A in Eurocode-8.

Site classification according to TBDY (2018)

The TBDY (2018) involves six site classes (ZA, Z B, Z C, ZD, ZE, and ZF) to identify the site-specific design spectra shown in Table 5.

As can be seen in Table 2, eight sites are classified as class ZD (30.77%), 16 as ZC (61.54%), and two as classified as ZB (7.69%), according to the $V_{s,30}$ criterion.

Site classification according to Rodriguez-Marek et al. (2001)

Rodriguez-Marek et al. (2001) proposed a geotechnical classification scheme based on results from the ground motion data analysis shown in Tables 5 and 6.

As seen in Table 2, 11 sites are classified as class D1 (42.3%), three as D-2 (11.54%), eight as D-3 (30.77%), one as C-1(3.85), one as C-2 (3.85), and two as C-3 (7.69%), according to the site period.

Site amplification of Hatay Province

Experimental amplification ratios (H/V) and predominant periods were obtained at 26 locations using the GÜRALP CMG 6TD with a three-component broadband velocity meter and a 12-volt power supply. The sensitivity of the seismometer sensor to ground motion varied in a wide frequency band from 0.033 to 50 Hz. Microtremor data were obtained in GCF (Guralp Compressed File) format. The three recorded components were viewed and edited with noise data SCREAM (Figure 9). The records were evaluated according to the single station method (H/V) by using Geopsy (SESAME Europe Project, 2004) software. Firstly, a trend analysis was applied to data for removing base-line

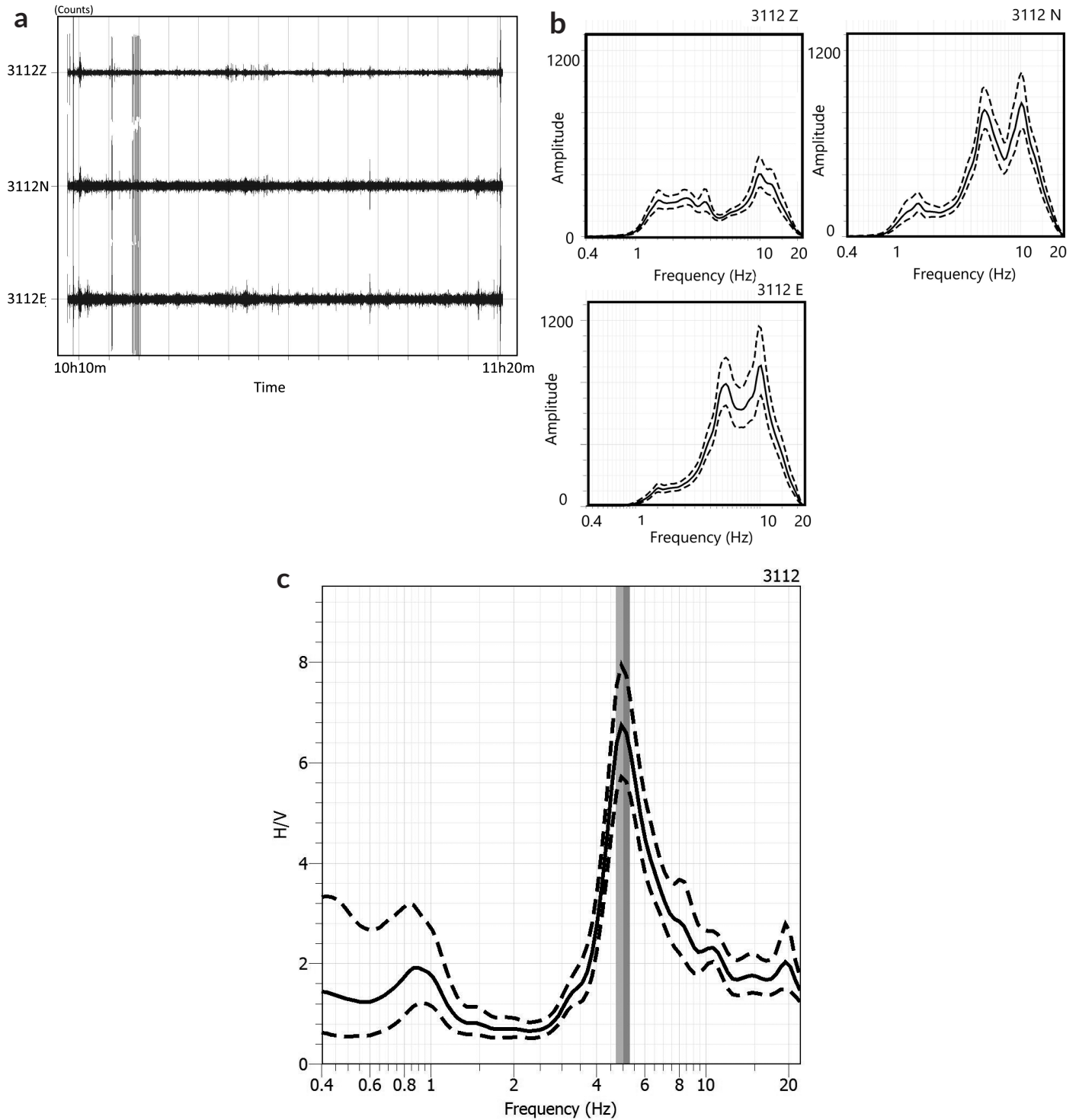


Figure 7. (a) Filtered time signal series, (b) The amplitude spectra of the three components microtremor data, the peak curves (average curve, black line), illustrate the corresponding resonant frequencies and (c) the H/V amplitude spectra. The dashed lines show the standard deviation of amplitude, and the two vertical gray areas show the peak frequency standard deviation domains.

trend and then a 5% rounded Cosine window was applied on the edges of the raw data to simulate sudden changes at both ends of the timeline. The amplitude of the side-oscillations that can be seen on the resultant spectra was reduced, and the data was filtered with a band-pass Butterworth filter between 1-20 Hz. Thus, the noises of very low and high frequencies are removed from the signals, and the frequency content of the microtremors is left behind. In evaluation of microtremor data, the number of windows is taken into consideration such that the number of distinct cycles in the entire record is greater than 200, the case

where the f_0 (dominant frequency) value is greater than or less than 0.5 Hz, (Table 2). In the evaluation of microtremor data; criteria such as number of windows, and the standard deviation values of the H/V curves were considered according to SESAME Project (Site. Effects Assessment Using Ambient Excitations, Contract No. EVG1-CT-2000-00026) The H/V peak amplitudes and predominant periods were interpreted according to SESAME (2004) criteria. The top 30 m site conditions were characterized in accordance with the NEHRP Provisions (BSSC 2003), Eurocode-8 (CEN2003), TBDY (2018) and

Table 1. Observed soil model of the 3112 station for theoretical H/V calculation

Compressional Wave Velocity, V_p (m/s)	Shear-Wave Velocity, V_s (m/s)	Quality factors P-velocity Q_p	Quality factors related with S-velocity Q_s	Density ρ (kg/m ³)	Thickness H(m)
431	217	5	1	1.8	0-1.43
431	219	15	5	1.9	1.43- 3.21
431	216	20	10	2.1	3.21- 5.44
431	207	25	20	2.2	5.44-8.23
431	203	30	30	2.5	8.23- 11.72
431	217	100	70	2.6	11.72-16.07
440	243				16.07-21.52
440	270				21.52-28.33
515	304				28.33-36.83
∞	∞				

Rodriguez-Marek et al. (2001), as shown in Table 2. The peak amplitudes of the stations (H/V) vary between 1.3-7.6 (Fig. 9a) and their dominant periods range from 0.23 to 3.3 s (Fig.9b).

Discussion

This article uses site responses, site amplification variations using microtremor data of 26 strong motion stations of AFAD in Hatay region. The shear wave velocities, V_{s30} , up to 30 m of depth vary between 221 and 597m/s at the 3112, 3113, 3114, 3115, 3116, 3117, 3119, 3120, and 3121 coded stations. These velocity values are almost the same as those determined by Ozmen et al. (2017) at the same stations. The difference between these two sets of velocity ranges between 0.07% and 2.95%. Büyüksaraç et al. (2014) have determined the velocity model of the underground in four stations. They determined the seismic velocities ranging between 380 and 470 m/s at a depth

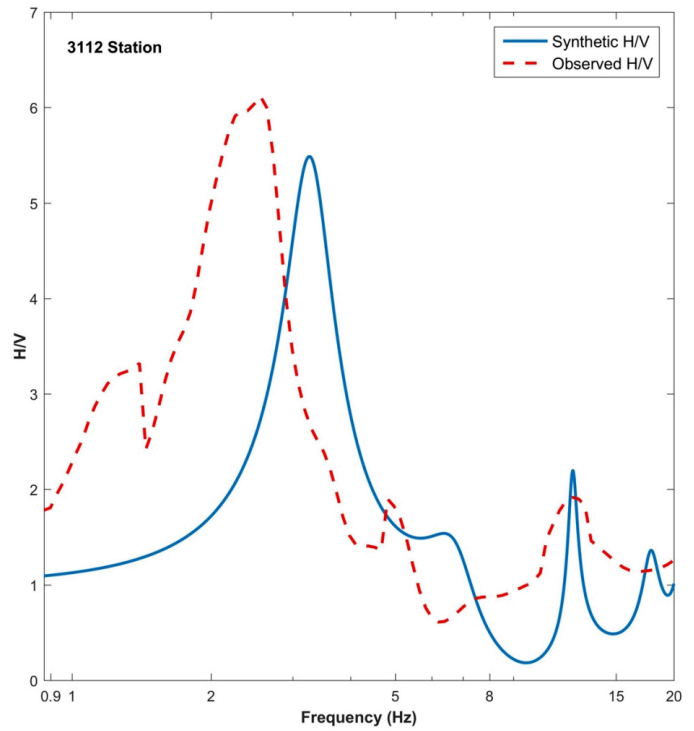


Figure 8. Synthetic and observed H/V curves at the 3112 station.

of 0-5m, between 320-480 m/s at a depth of 5-15 m, and between 470-750 m at a depth of 15-25 m. This data are in good agreement with the velocity data obtained in this study (Figs. 5c and 6c). In addition, the soil amplification was calculated as 1.5 in periods of 0.4sec and 0.5sec and 2.0 in the other two stations in 0.25sec and 0.4sec periods, which approximately correspond to the values

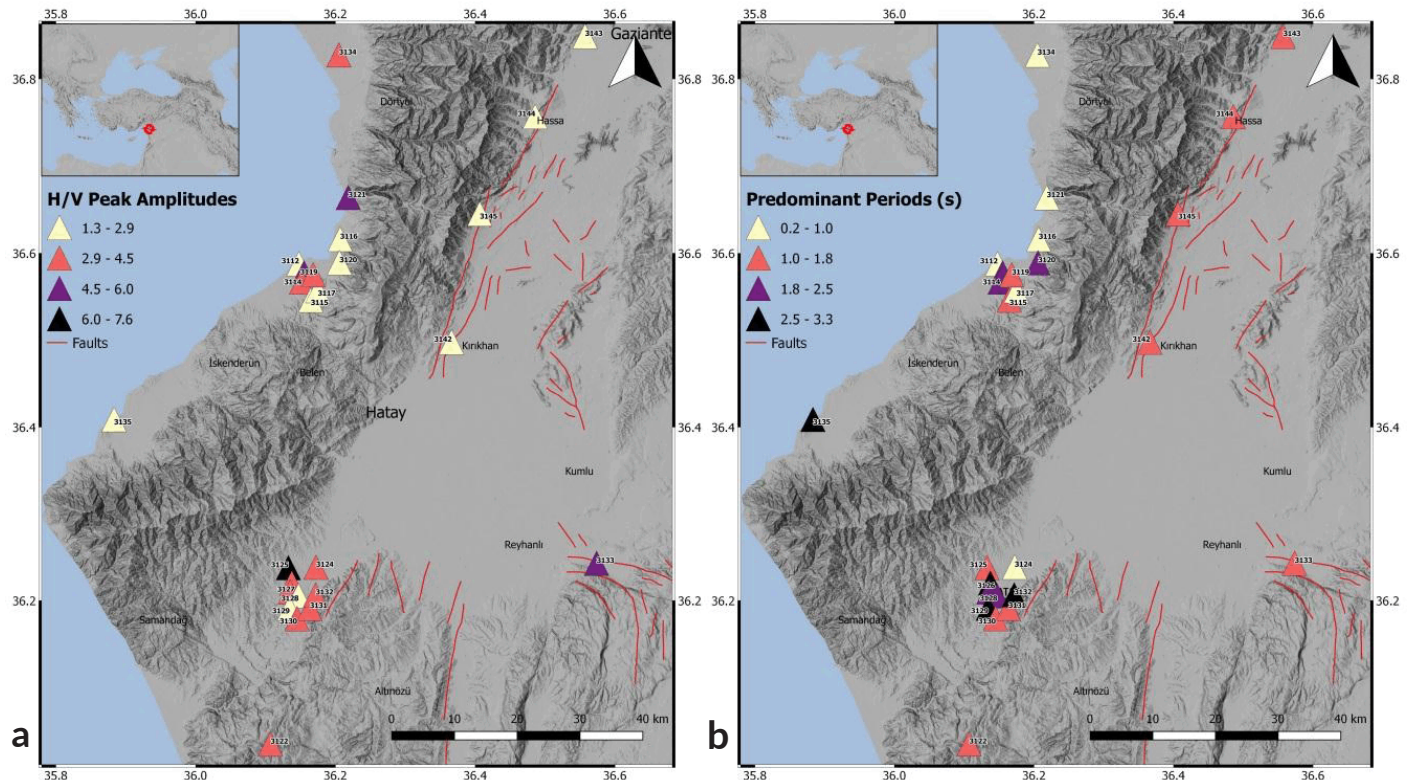


Figure 9. (a) H/V peak amplitudes, (b) pre-dominant periods

Table 2. Combined data set of study in Hatay province

No	Station Code	Lat.	Lon.	Vs ₃₀ (m/s)	H/V Peak Amplitudes	T ₀ (s)	NEHRP	E-Code-8	TBDY	RM-2001	Lithology
1	3112	36.59	36.15	233	1.3	0.7	D	C	ZD	C-3	Unidentified Quaternary Alluvium
2	3113	36.58	36.16	221	4.8	1.85	D	C	ZD	D-3	Basalt
3	3114	36.57	36.15	215	4.1	2.5	D	C	ZD	D-3	Unidentified Quaternary Alluvium
4	3115	36.55	36.16	424	2.5	1.1	C	B	ZC	D-1	Unidentified Quaternary Alluvium
5	3116	36.62	36.21	781	1.6	0.23	B	B	ZB	D-1	Unidentified Quaternary Alluvium
6	3117	36.56	36.17	597	2.67	0.24	C	B	ZC	C-1	Clastic and Carbonates Rocks
7	3119	36.58	36.17	374	3.9	1.51	C	B	ZC	D-1	Clastic and Carbonates Rocks
8	3120	36.59	36.21	455	2.87	1.9	C	B	ZC	D-1	Clastic and Carbonates Rocks
9	3121	36.66	36.22	271	5.5	0.55	D	C	ZD	C-3	Clastic and Carbonates Rocks
10	3122	36.03	36.11	1011	3.1	1.45	B	A	ZB	C-2	Clastic and Carbonates Rocks
11	3124	36.24	36.17	283	4.1	0.81	D	C	ZD	D-1	Clastic and Carbonates Rocks
12	3125	36.24	36.13	448	7.6	1.38	C	B	ZC	D-1	Clastic and Carbonates Rocks
13	3126	36.22	36.14	350	3.1	2.8	D	C	ZD	D-3	Clastic and Carbonates Rocks
14	3127	36.21	36.14	404	2.9	1.96	C	B	ZC	D-3	Clastic and Carbonates Rocks
15	3128	36.21	36.15	329	2.36	1.96	D	C	ZD	D-3	Clastic and Carbonates Rocks
16	3129	36.19	36.13	447	2.7	3.3	C	B	ZC	D-3	Clastic and Carbonates Rocks
17	3130	36.18	36.15	447	4.2	1.4	C	B	ZC	D-1	Clastic and Carbonates Rocks
18	3131	36.19	36.16	567	4.2	1.3	C	B	ZC	D-1	Clastic and Carbonates Rocks
19	3132	36.21	36.17	377	3.2	2.94	C	B	ZC	D-3	Clastic and Carbonates Rocks
20	3133	36.24	36.57	471	4.6	1.19	C	B	ZC	D-2	Clastic and Carbonates Rocks
21	3134	36.83	36.20	374	4.1	0.87	C	B	ZC	D-2	Clastic and Carbonates Rocks
22	3135	36.41	35.88	460	2.5	2.9	C	B	ZC	D-3	Clastic and Carbonates Rocks
23	3142	36.50	36.37	191	1.6	1.06	D	C	ZD	D-2	Clastic and Carbonates Rocks
24	3143	36.85	36.56	444	2.2	1.42	C	B	ZC	D-1	Alluvium Fan
25	3144	36.76	36.49	485	2.2	1.1	C	B	ZC	D-1	Basalt
26	3145	36.65	36.41	533	2.2	1.66	C	B	ZC	D-1	Alluvium Fan

that we determined. Over et al. (2001) found the average Vs velocities from the REMI studies 413m/s at 0-13m of depth, 420m/s at 13-33m, 560m/s at 33-62m, and 537m/s at about 100 m. These values are very close to the values that we determined by applying the MASW and REMI methods. They also calculated the dominant soil periods between 0.2sec and 0.8sec and site amplification

values between 1.1 and 1.8, which correspond to what we found. The sites were classified in accordance with NEHRP Provisions (BSSC, 2003), Eurocode 8 (CEN, 2003), TBDY (Turkish Building Earthquake Regulations, 2018), and Rodriguez-Marek et al. (2001), and tabulated in Table 2. The site classes were found at the stations located to the west of the Amanos Mountains as C and D

Table 3. Site class definitions in NEHRP provisions (BSSC 2003)

Site Class	$V_{s,30\text{ m}}$ (m/s)
A	$V_{s,30\text{ m}} > 1,500$
B	$760 < V_{s,30\text{ m}} \leq 1,500$
C	$360 < V_{s,30\text{ m}} \leq 760$
D	$180 \leq V_{s,30\text{ m}} \leq 360$
E	$V_{s,30\text{ m}} < 180$
	Any profile with more than 3 m of soft clay defined as soil with $PI > 20$, $w \geq 40\%$ and $S_u < 25$ kPa

Table 4. Site class definitions in Eurocode-8 (CEN 2003)

Site Class	$V_{s,30\text{ m}}$ (m/s)
A	$V_{s,30\text{ m}} > 800$
B	$360 < V_{s,30\text{ m}} \leq 800$
C	$180 \leq V_{s,30\text{ m}} \leq 360$
D	$V_{s,30\text{ m}} < 180$
E	A soil profile consisting of a surface alluvium layer with V_s in the range given for sites of types C or D, with thickness varying between 5 and 20 m and which is underlain by stiffer material with $V_s > 800$ m/s
S1	Deposits containing a layer of soft clays/silts with a high plasticity index ($PI > 40$) and high water content with $V_s < 100$ m/s or $10 < S_u < 20$ kPa and at least 10 m thick
S2	Deposits of liquefiable soils, of sensitive clays, or any other soil profile not included in types A-E or S1

Table 5. Turkey Earthquake Building Regulations (TBDY-2018)

Local Soil Classes	Soil Type	V_{s30} [m/s]
ZA	Strong, hard rocks	> 1500
ZB	Weak altered, medium strong rocks	760-1500
ZC	Very stiff sand, gravel and hard clay layers or latered, very cracked weak rocks	360-760
ZD	Medium-hard sand, gravel or very hard clay layers	180-360
ZE	Soft sand, gravel or soft-hard clay layers or profiles containing a soft clay layer ($c_u < 25$ kPa) of a total thickness of 3 meters providing conditions of $PI > 20$ and $w > 40\%$	< 180

according to NEHRP and B and C according to Eurocode-8. In both systems, the ground class was calculated as B at Station 3116. Soil classes were the same in the NEHRP and TBDY-2018 systems. Soil classifications obtained in NEHRP and TBDY systems were similar. H/V peak amplitude values were calculated as 2.2 at Stations 3143, 3144, and 3145. The H/V values of the stations coded 3123 and 3125 are 3.9 and 4.6, respectively. The H/V value was calculated between 3.9 and 4.6 for Stations 3113, 3114, 3119, 3124, 3130, 3131, 3133, and 3134 and between 1.3 and 3.3 for other stations. The dominant periods (T_0) of the stations were between 0.23sec (at Station 3112) and 3.3sec (at Station 3129).

Table 6. Site classes proposed by Rodriguez-Marek et al. (2001)

Site	Description	Site Period	Comments
A	Hard Rock	<0.1 s	Hard, strong, intact rock ($V_s \geq 1500$ m/s)
B	Rock	<0.2 s	Most "unweathered" California rock cases ($V_s \geq 760$ m/s or <6 m of soil)
C-1	Weathered/Soft Rock	<0.4 s	Weathered zone >6 m and <30 m ($V_s > 360$ m/s increasing to > 700 m/s)
C-2	Shallow Stiff Soil	<0.5 s	Soil depth >6 m and <30 m
C-3	Intermediate Depth Stiff Soil	<0.8 s	Soil depth >30 m and < 60 m
D-1	Deep Stiff Holocene Soil, either S (Sand) or C (Clay)	<1.4 s	Soil depth >60 m and < 200 m. Sand has low fines content (< 15%) or nonplastic fines ($PI < 5$). Clay has high fines content (> 15%) and plastic fines ($PI > 5$).
D-2	Deep Stiff Pleistocene Soil, S (Sand) or C (Clay)	<1.4 s	Soil depth >60 m and < 200 m. See D1 for S or C sub- categorization.
D-3	Very Deep Stiff Soil	<2.0 s	Soil depth >200 m
E-1	Medium Depth Soft Clay	<0.7 s	Thickness of soft clay layer 3 m to 12 m
E-2	Deep soft clay level	<1.4 s	Thickness of soft clay layer >12 m
F	Special, e.g. Potentially Liquefiable Sand or Peat	= 1.0 s	Holocene loose sand with high water table ($z_w \leq 6$ m) or organic peat

Conclusion

In this study, the subsurface soil condition and experimental site amplification ratios at the strong motion stations of AFAD in the province of Hatay were investigated through geophysical methods including seismic refraction, MASW, REMI, and microtremor surveying. The studies were carried out at 26 strong motion stations to evaluate the site effects and seismic hazard of the Hatay region. The shear-wave velocity profiles of the upper 30m of the sites were determined with MASW and ReMi techniques. Transfer functions (maximum H/V amplitude ratios) and predominant periods were obtained at the same locations by applying microtremor studies. The shear-wave velocities determined with the MASW technique were compared with those obtained employing the ReMi technique. The site class and soil amplification ratio as well as the dominant period of each site are tabulated in Table 2.

The peak frequency of the H / V ratio in a field can be used to create a standard H / V response spectrum, which is a good diagnosis of the field condition. The peak amplitude of the H/V function varies between 1.3 and 5.5. The shape of the standard H / V ratio curve is very similar across regions. V_{s30} values (191-1011 m/s) corresponding to these peaks show scattering because the studied environments are in a very complex structure.

Two types of regions are recognized based on their dominant period, T_0 , characteristics: (1) T_0 value, respectively, in Hatay region is generally higher than 0.87sec and (2) in İskenderun region generally lower than 2.5sec.

The database supported by the precise descriptions of site conditions presented here will provide valuable information and will contribute to further

development of methods to assess the relationship between site conditions and strong motion parameters.

Acknowledgment

This study was funded and supported by the AFAD (Disaster and Emergency Management Presidency) National Earthquake Research Program (UDAP-G-15-04) within the scope of the “Determination of Soil Parameters of Turkish Strong Motion Recording Stations Project.”

REFERENCES

- Akbaş, B., Akdeniz, N., Aksay, A., Altun, I., Balcı, V., Bilginer, E., Bilgiç, T., Duru, M., Ercan, T., Gedik, I., Günay, Y., Güven, I.H., Hakyemez, H.Y., Konak, N., Papak, I., Pehlivan, S., Sevin, M., Şenel, M., Tarhan, N., ... Yurtsever, A. (2002). *Turkey Geology Map*. General Directorate of Mineral Research and Exploration Publications, Ankara.
- Alçık, H., Gürbüz, C. & Uçer, S. (1995). Kadıköy ve Üsküdar bölgelerinde yapılan mikro-tremor ölçümleri ile mikrobölgeleme. *Jeofizik Dergisi*, 9(1), 235-245.
- Ambraseys, N. N., Durukal, E. & Free, M. (1993). *Re-evaluation of strong-motion data from Turkey*. Imperial College of Science, Technology and Medicine, Civil Engineering Department.
- Aydan, O. & Hasegür, Z. (1997). *The characteristics of acceleration waves of Turkish earthquakes*. Proceedings of the 4th national conference on earthquake engineering, Turkish National Committee of Earthquake Engineering, Ankara, Turkey, 30-37.
- Bayülke, N. (1982). The 19 August 1976 Denizli, Turkey, earthquake: evaluation of the strong motion accelerograph record. *Bulletin of the Seismological Society of America*, 72(5), 1635-1649.
- Beyen, K., Erdik, M., Mazmanoğlu, C. & Ekmekçiöğlü, Z. (2003). Antakya'nın geçmişten günümüze sismik aktivitesi ve yapılması gerekenlerin bir uluslararası konferansın ışığında değerlendirilmesi. *Engineering Report of Turkey*, 423(1), 51-53.
- BSSC (Building Seismic Safety Council) (2003). *Recommended Provisions for Seismic Regulations for New Buildings and Other Structures and Accompanying Commentary and Maps*. FEMA 450, Chapter 3, 17-49.
- Büyüksaraç, A., Over, S., Genç, M. C., Bıkçe, M., Kacın, S. & Bektaş, O. (2014). Estimating shear wave velocity using acceleration data in Antakya (Turkey). *Earth Sciences Research Journal*, 18(2), 87-98.
- CEN (European Committee for Standardization) (2003). Design of structures for earthquake resistance – part 1: general rules, seismic actions and rules for buildings, EN-1998- 2003, European Committee for Standardization, Brussels.
- Ceken, U. & Polat, O. (2014). Investigation of the Local Soil Effects at the New Strong-Motion Array (MATNet) in Hatay-Kahramanmaraş Region, Turkey, AGU Fall Meeting, 15-19 December 2014, San Francisco, ABD, Nr: T13C-4660, 232 pp.
- Dikmen, U. & Mirzaoglu, M. (2005). The seismic microzonation map of Yenisehir-Bursa, NW of Turkey by means of ambient noise measurements. *Journal of the Balkan Geophysical Society*, 8(2), 53-62.
- Durukal, E., Alpay, Y., Biro, T., Mert, A. & Erdik, M. (1998). *Analysis of strong motion data of the 1995 Dinar*. In: Turkey earthquake, second Japan-Turkey workshop: earthquake disaster prevention research in Turkey, February, 23-25.
- Emre, O., Duman, T. Y., Ozalp, S., Elmacı, H., Olgun, S. & Saroğlu, F. (2013). Scale 1/1.125.000 Turkey live fault map. General Directorate of Mineral Research and Exploration special publications series-30, Ankara, Turkey.
- Erdik, M. (1984). Report on the Turkish earthquake of October 30, 1983. *Earthquake Spectra*, 1(1), 151-172.
- Ergin, M., Aktar, M. & Eyidoğan, H. (2004). Present-day seismicity and seismotectonic of the Cilician Basin: Eastern Mediterranean Region of Turkey. *Bulletin of the Seismological Society of America*, 94(3), 930-939.
- Gülkan, P., Çeken, U., Çolakoğlu, Z., Uğraş, T., Kuru, T., Apak, A., Anderson, J. G., Sucuoğlu, H., Çelebi, M., Akkar, D. S., Yazgan, U. & Denizlioğlu, A. Z. (2007). Enhancement of the national strong-motion network in Turkey. *Seismological Research Letters*, 78(4), 429-438.
- Herak, M. (2008). ModelHVSR—A Matlab tool to model horizontal-to-vertical spectral ratio of ambient noise. *Computers & Geosciences*, 34(11), 1514-1526.
- Horoz, Ş. (2008). Adana-Antakya-Kahramanmaraş arasındaki bölgenin depremselliğinin “b” parametresi ile incelenmesi ve risk analizi. Ph.D. Thesis, Cumhuriyet University, Institute of Science, Department of Geophysics, Sivas, Turkey.
- Inan, E., Colakoglu, Z., Koc, N., Bayülke, N. & Coruh, E. (1996). *Earthquake catalogs with acceleration records from 1976 to 1996*. General Directorate of Disaster Affairs, Earthquake Research Department, Ankara, Turkey, 98 pp.
- Kalafat, D., Güneş, Y., Kara, M., Deniz, P., Kekovaht, K., Kuleli, H. S., Gülen L., Yılmaz M. & Ozel, N. M. (2007). *A Revised and extended earthquake catalogue for Turkey since 1900 (MC4.0)*. Bogazici University library cataloging, ISBN 978-975-518-281-0, Istanbul, Turkey, 450 pp.
- Kalkan, E. & Gülkan, P. (2004). Site-dependent spectra derived from ground motion records in Turkey. *Earthquake Spectra*, 20(4), 1111-1138.
- Korkmaz, H. (2006). Antakya'da zemin özellikleri ve deprem etkisi arasındaki ilişki. *Coğrafi Bilimler Dergisi*, 4(2), 49-66.
- Kurtuluş, C. & Bozkurt, A. (2016). Integration of geophysical and geotechnical investigations for Çayırhan town. *Journal of Applied Earthscience*, 8(2), 15-27.
- Livaoğlu, H., & Sertçelik, F. (2017). *A Practical Solution for Detecting the Bedrock Depth beneath the Strong Ground Motion Stations: A Case Study for Kocaeli Province (Turkey)*. 9th Congress of the Balkan Geophysical Society, Antalya, Turkey.
- Livaoğlu, H., & İrmak, T.S., (2017). An empirical relationship between seismic bedrock depth and fundamental frequency for Değirmendere, (Kocaeli-Turkey). *Environmental Earth Sciences*, 76(2), 681 pp.
- Louie, J. N. (2001). Faster, better: shear-wave velocity to 100 meters depth from refraction microtremor arrays. *Bulletin of the Seismological Society of America*, 91(2), 347-364.
- Ongun, E. R. (2010). İzmir Balçova kuvvetli yer hareketi istasyonu zemin şartlarının jeofizik yöntemlerle araştırılması, Msc Thesis, Dokuz Eylül University. Institute of Science, İzmir.
- Over, S., Büyüksaraç, A., Bektaş, O. & Filazi, A. (2011). Assessment of potential seismic hazard and site effect in Antakya (Hatay Province), SE Turkey. *Environmental Earth Sciences*, 62(2), 313-326.
- Ozalaybey, S., Ergin, M., Aktar, M., Tapirdamaz, C., Biçmen, F. & Yörük, A. (2002). The 1999 Izmit earthquake sequence in Turkey: seismological and tectonic aspects. *Bulletin of the Seismological Society of America*, 92(1), 376-386.
- Ozmen, O. T., Yamanaka, H., Alkan, M. A., Çeken, U., Oztürk, T. & Sezen, A. (2017). Microtremor array measurements for shallow s-wave profiles at strong-motion stations in Hatay and Kahramanmaraş provinces, Southern Turkey. *Bulletin of the Seismological Society of America*, 107(1), 445-455.
- Park, C. B., Miller, R. D. & Xia, J., (1999). Multichannel analysis of surface waves. *Geophysics*, 64(3), 800-808.
- Polat, O. & Çeken, U. (2014). Investigation of the local soil effects at the new strong-motion array (MATNet). In: Hatay-K (Ed.) Maras region, Turkey, American Geophysical Union, Fall Meeting Abstracts, 15-19 December, San Francisco-USA, Nr:T13C-4660, 232 pp.
- Rathje, E. M., Stokoe, K. H. & Rosenblad, B. (2003). Strong motion station characterization and site effects during the 1999 earthquakes in Turkey. *Earthquake Spectra*, 19(3), 653-675.
- Reilinger, R. E., McClusky, S. C., Oral, M. B., King, R. W., Toksoz, M. N., Barka, A. A., Kinik, I., Lenk, O. & Sanli, I. (1997). Global Positioning System measurements of present-day crustal movements in the Arabia-Africa-Eurasia plate collision zone. *Journal of Geophysical Research: Solid Earth*, 102(B5), 9983-9999.

- Rodriguez-Marek, A., Bray, J. D. & Abrahamson, N. A. (2001). An empirical geotechnical site response procedure. *Earthquake Spectra*, 17(1), 65-87.
- Sandikkaya, M. A. (2008). Site classification of national strong-motion recording sites. MSc thesis, Civil Engineering Department, Middle East Technical University, Ankara, Turkey, 98-106.
- Sandikkaya, M. A., Yılmaz, M. T., Bakır, B. S. & Yılmaz, O. (2010). Site classification of Turkish national strong-motion stations. *Journal of Seismology*, 14(3), 543-563.
- SESAME (2004). Guidelines for the implementation of the H/V spectral ratio technique on ambient vibrations measurements, processing and interpretation, SESAME, European project, WP12, Deliverable D23.12, December.
- TDBY Türkiye (2018). Deprem ve Bina Yönetmeliği, Resmî Gazete, Sayı:30364, 18 Mart.
- Tarı, U., Tüysüz, O., Genç, Ş. C., İmren, C., Blackwell, B. A., Lom, N., Tekeşin, O., Usküplü, S., Erel, L., Altok, S. & Beyhan, M. (2013). The geology and morphology of the Antakya graben between the Amik Triple Junction and the Cyprus Arc. *Geodinamica Acta*, 26(1-2), 27-55.
- Tsai, N. C. (1970). A note on the steady-state response of an elastic half-space. *Bulletin of the Seismological Society of America*, 60(3), 795-808.
- Tsai, N. C. & Housner, G. W. (1970). Calculation of surface motions of a layered half-space. *Bulletin of the Seismological Society of America*, 60(5), 1625-1651.
- Ulusay, R., Tuncay, E., Sönmez, H. & Gökçeoğlu, C. (2004). An attenuation relationship based on Turkish strong motion data and iso-acceleration map of Turkey. *Engineering Geology*, 74(3), 265-291.
- Xia, J., Miller, R. D. & Park, C. B. (1999). Estimation of near-surface shear-wave velocity by inversion of Rayleigh waves. *Geophysics*, 64(3), 691-700.
- Yılmaz, O., Savaşkan, E., Bakır, B. S., Yılmaz, M. T., Eser, M., Akkar, S., Tüzel, B., İravul, Y., Özmen, O., Denizlioğlu, Z., Alkan, A. & Gürbüz, M. (2008). Shallow seismic and geotechnical site surveys at the Turkish national grid for strong-motion seismograph stations. In: 14th world conference on earthquake engineering, Beijing, China.
- Zaré, M. & Bard, P.Y. (2002). Strong motion dataset of Turkey: data processing and site classification. *Soil Dynamics and Earthquake Engineering*, 22(8), 703-718.
- Zhang, J. & Toksöz, M. N. (1998). Nonlinear refraction travelttime tomography. *Geophysics*, 6, 1726 - 1737.